Fast Radon Transform for Detection of Seismic Reflections

Peter A. TOFT and Kim V. HANSEN†

Electronics Institute, Technical University of Denmark, DK-2800 Lyngby, Denmark,
Tel/Fax +45 45 93 42 07/42 88 01 17, E-Mail: ptoft@ei.dtu.dk
†Ødegaard & Danneskiold-Samsøe ApS, Kroghsgade 1, DK-2100 København Ø, Denmark,
Tel/Fax +45 35 26 60 11/35 26 50 18, E-Mail: kvh@oedan.dk

Abstract. A new method for fast detection of seimic reflections is proposed. Generally the method can be viewed as a curve matching method for images with a specific structure. In this paper the method is applied to seismic signals assembled to constitute an image in which the investigated reflections produce hyperbolic curves.
The idea of the proposed method is to estimate the reflection curves by combining the multipulse technique and the FCE-algorithm [1]. The FCE-algorithm is an algorithm used for fast curve estimation within binary images. The foundation of the FCE-algorithm is the composition of a pre-condition map which significantly reduces the computational cost compared to the traditional generalized Radon transform.
The proposed method is succesfully applied for detection of hyperbolic reflection curves within CMP-gathers.

1 Introduction

The seismic industry has developed a method of sampling seismic signals that gives multiple coverage. The recording geometry of seismic acquisition results in signals having the same mid point between source and receiver [2]. The set of signals corresponding to the same mid point is called a CMP-gather (common mid point gather).

Without any assumptions concerning the seismic signal processing, two facts of the CMP-gather are noticed. Almost the same short signal sequence (the wavelet) is observed several times within each trace and the same short signal sequence is seen along curves within several traces. These two facts form the basis of the reflection detection. The reflections represent information concerning the geological structure of the subsurface. If the subsurface is assumed to be horizontally layered it can be shown [2] that the shape of the reflection curves are hyperbolas, described by the normal moveout equation. Currently, reflections are identified from CMP-gathers by using velocity analysis succeeded by a manual picking of primary reflections. This procedure is inconvenient due to the computational burden and the required interpretation performed by an expert. These facts motivate the development of an automatic reflection identification procedure.

The key idea of the proposed method for detection of reflection curves is to combine the multipulse technique with the FCE-algorithm [1]. The multipulse technique is used to identify the wavelet in each trace, and the FCE-algorithm is used to coordinate the estimation of the reflection sequence.

The proposed method works on CMP-gathers, shot-gathers, and other types of gathers.

2 The Multipulse Technique

Recently, the multipulse excited speech coding technique, which was originally proposed by Atal *et al.* [3], has been suggested for seismic deconvolution by Cookey *et al.* [4]. Basically, the multipulse model for speech assumes the speech signal to be a result of several impulses modulated by the shape of the vocal tract filter. Within seismic deconvolution models, the input signal is often modeled as an all-pole impulse and the layered earth reflectivity model is considered as an impulse train.

Fundamentally, the reflections within each trace are estimated by minimizing the mean square error between the recorded and the modeled signal. The method is characterized by successive estimation of a pre-defined number of reflections. Thus, the multipulse technique can be used to map seismic signals in a CMP-gather into a binary image, where the image value is set to one in case of a reflection and otherwise is set to zero.

3 Fast Hyperbola Estimation

A recurring problem in computer image processing is the identification of curves with specific shapes. In digital image processing a special variant of the generalized Radon transform [5], called the Hough transform [6, 7], is used for detection of curves in images. The Hough transform detects specific values of parameters, which characterize these curves. Spatially extended curves are transformed to produce spatially compact features in a space of possible parameter values. Thus, the generalized Radon transform converts a difficult global detection problem in the image space into a more easily solved local peak detection problem in a parameter space.

The foundation of the FCE-algorithm is the composition of a pre-condition map which reduces the computational costs of the traditional generalized Radon transform. The pre-condition map is composed of irregular regions in the parameter domain which represent the interesting areas of the parameter domain, i.e., the regions of the parameter domain which contain peaks representing curves. Initially, the FCE-algorithm estimates the pre-condition map and subsequently applies a traditional generalized Radon transform within the regions specified by the pre-condition map. To generate the pre-condition map a fast mapping procedure named *image point mapping* (*IPM*) is presented. As *IPM* maps image points into the corresponding parameter values in the parameter domain, it can profit by image points with value zero.

Assuming a horizontally layered subsurface the reflection curves within a CMP-gather are described by the normal moveout equation [2]

$$t_n = \phi(\kappa_x; t_{0,z}, \sigma_s) = \sqrt{t_{0,z}^2 + (\sigma_s \kappa_x)^2} \qquad (1)$$

where t_n denotes the two way travel time, $t_{0,z}$ the zero offset two way travel time, κ_x the offset, and σ_s the slowness. The subscripts denote corresponding discrete variables.

In this paper a linear sampling of the variables is chosen according to

$$\xi_i = \xi_{i,j} = \xi_{i,low} + j_i \, \Delta\xi_i, \quad j_i = 0, 1, \ldots, J_i - 1 \quad (2)$$

where j_i is a discrete variable, $\xi_{i,low}$ denotes the lower limit, $\Delta\xi_i$ the sampling interval and J_i is the number of samples of ξ_i.

Substitution of the linear sampling into eq. (1) gives

$$\begin{aligned} n &= \phi_d(x; z, s) \\ &= round((\phi(\kappa_x; t_{0,z}, \sigma_s) - t_{low})/\Delta t) \end{aligned} \qquad (3)$$

where $round(\cdot)$ rounds to the closest integer.

Let $d(x, n)$ denote a discrete image and let $\mathcal{D}(z, s)$ denote the discrete generalized Radon transform of $d(x, n)$ defined by

$$\mathcal{D}(z, s) = \sum_{x=0}^{X-1} d(x, \phi_d(x; z, s)) \qquad (4)$$

Normally, the use of rounding instead of e.g., linear interpolation will not cause problems. However, interpolation can easily be incorporated in eq. (3) and (4).

The discrete generalized Radon transform can be rewritten as

$$\mathcal{D}(z, s) = \sum_{x=0}^{X-1} \sum_{n=0}^{N-1} d(x, n) \, \delta(n - \phi_d(x; z, s)) \qquad (5)$$

where $\delta(\cdot)$ denotes the Kronecker delta function.

Eq. (5) shows that each image point (x, n) is transformed into a parameter curve where $\phi_d(x; z, s) = n$. Thus mapping of image points with zero value is needless, as they will not contribute to $\mathcal{D}(z, s)$.

Inversion of eq. (1) and insertion of the linear sampling relations of the variables leads to

$$\begin{aligned} z &= \Omega_d(x, n; s) \\ &= round((\sqrt{t_n^2 - (\sigma_s \kappa_x)^2} - t_{0,low})/\Delta t_0) \end{aligned} \qquad (6)$$

Based on eq. (5) and (6) the estimation scheme *IPM* is defined. This can be summarized as

1. Initialize $\mathcal{D}(z, s) = 0$ for all (z, s)
2. For all image points $d(x, n)$ with a value different from zero do
   For all possible s do
   $\mathcal{D}(\Omega_d(x, n; s), s) := \mathcal{D}(\Omega_d(x, n; s), s) + d(x, n)$

In the hyperbolical case eq. (6) will describe an ellipse. This causes a problem for $|\Omega_d(x, n; s) - \Omega_d(x, n; s-1)| > 1$, which results in a perforated ellipse. This perforation problem can be eliminated simply by adding $d(n, x)$ to $\mathcal{D}(z, s)$ for the parameter values skipped between two subsequent parameter vectors. Using *IPM* the ellipses from points lying on a hyperbola might not intersect in one parameter combination, but will spread out. This problem can be eliminated using a sparse sampled parameter domain. However, *GRT* requires a dense sampling of the parameter domain to ensure that all hyperbolas are detectable.

3.1 *The FCE-algorithm*

From the characteristics of *GRT* and *IPM* it is possible to construct a <u>f</u>ast <u>c</u>urve parameter <u>e</u>stimation algorithm, the *FCE-algorithm* [1], that simultaneously estimates all curve parameters within a sparse binary image.

The FCE-algorithm can be summarized as follows:

1. Design the discrete parameter domain, i.e., choose $\xi_{i,low}$, J_i and $\Delta\xi_i$, $\xi_i \in \{t_{0,z}, \sigma_s\}$.
2. Design a reduced parameter domain for *IPM* by choosing

$$\begin{aligned} J_i' &= ceil\left(\frac{J_i}{2v_{\xi_i} + 1}\right) && (7) \\ \xi_{i,low}' &= \xi_{low} + v_{\xi_i}\Delta\xi_i && (8) \\ \Delta\xi_i' &= (2v_{\xi_i} + 1)\Delta\xi_i && (9) \end{aligned}$$

where $ceil(\cdot)$ rounds to the nearest upper integer. Then use *IPM* to estimate $\mathcal{D}_m(z', s')$ as

$$\mathcal{D}_m(z', s') = IPM\{d(x,n)\} \tag{10}$$

3. Use a threshold to remove all insignificant parameter combinations. A suitable choice could be

$$\mathcal{D}_t(z', s') = \mu(\mathcal{D}_m(z', s') - \lambda_1 \; X) \tag{11}$$

where X denotes the number of image lines, λ_1 a fraction defining the significance level, and $\mu(\cdot)$ the Hamilton step function.

4. Resample the parameter domain to obtain $\mathcal{D}_r(z, s)$. The resampling process can be written as

$$\begin{aligned} \mathcal{D}_r(z,s) &= \mathcal{D}_t(z', s') & (12) \\ j_i' &= round\left(\frac{j_i - v_{\xi_i}}{2v_{\xi_i} + 1}\right) & (13) \end{aligned}$$

This gives a full size parameter domain where the interesting regions have value one while all other regions have value zero.

5. Use *GRT* to estimate $\mathcal{D}(z, s)$ in the regions of the parameter domain where $\mathcal{D}_r(z, s)$ is not equal to zero.

$$\mathcal{D}(z,s) = GRT\{d(x,n) | \, \mathcal{D}_r(z,s) \neq 0\} \tag{14}$$

6. As in step three use the threshold function with significance level λ_2. After the thresholding all points in the parameter domain having a value different from zero represent curve parameters.

The significance levels λ_1 and λ_2 must be chosen in accordance with the properties of the image. In general λ_1 and λ_2 are not critical. A suitable choice of λ_1 and λ_2 could be $0.1 - 0.7$ and $0.4 - 0.8$, respectively. There are two reasons for a low acceptance level in step three. Firstly, *IPM* has a tendency to blur in the parameter domain and secondly, only regions of the parameter domain ensured not to contain image curves must be left out. A higher significance level in step six (λ_2) is justified by the required certainty for correct curve identification.

4 Numerical Example

To illustrate the performance of the presented method for determination of reflection curves within CMP-gathers a numerical example is given.

Consider a CMP-gather where the image values are represented by continuous values. The CMP-gather can be mapped into a binary image $d(x, n)$ by deconvolution based on the multipulse technique [4, 8]. Figure 1.left shows a synthetic CMP-gather and Figure 1.right the thresholded image obtained by multipulse technique deconvolution. The CMP-gather is composed of seven reflection curves. Concerning the deconvolution fifteen reflections are chosen to be estimated within each trace, which implies that eight erroneous reflections within each trace have been found. These eight reflection will act as uncorrelated noise.

Next, Figure 2 shows the parameter domain obtained by use of *IPM*, where $v_{t_0} = 2$ and $v_\sigma = 4$. Figure 3 shows the parameter domain achieved by applying *GRT* in the parameter domain region specified by the thresholded and resampled parameter domain obtained by *IPM*. Within the thresholding process a significance level of $\lambda_1 = 0.5$ has been used. Finally, Figure 4 shows the identified reflection hyperbolas, where a significance level of $\lambda_2 = 0.8$ has been used in the thresholding. As seen all reflection curves have been found.

5 Conclusion

A new method for fast detection of seismic reflections is presented. Generally, the method can be viewed as a curve matching method for images with a specific structure.

The foundation of the proposed method is to estimate the reflection curves by combining the multipulse technique [3, 4] and the FCE-algorithm [1]. The multipulse technique is used for wavelet identification within each trace, and the FCE-algorithm is used to coordinate the wavelet identification between the individual traces.

The proposed method is succesfully applied for detection of hyperbolic reflection curves within CMP-gathers.

References

[1] K. V. Hansen and P. A. Toft, "Fast Curve Estimation Using Pre-Conditioned Generalized Radon Transform," Submitted for publication, August 1993.

[2] W. A. Schneider, "The Common Depth Point Stack," *Proc. IEEE*, vol. 72, no. 10, pp. 1238–1254, Oct. 1984.

[3] B. S. Atal and J. R. Remde, "A New Model of LPC Excitation for Producing Natural-Sounding Speech at Low Bit Rates," *IEEE ICASSP*, vol. 1, 1982, pp. 614–617.

[4] M. Cookey, H. J. Trussel and I. J. Won, "Seismic Deconvolution by Multipulse Methods," *IEEE Trans. ASSP*, no. 1, vol. 38, pp. 156–160, Jan. 1990.

[5] J. Radon, "Über die Bestimmung von Funktionen durch ihre Integralwerte längs gewisser Mannigfaltigkeiten," *Ber. Ver. Sächs. Akad. Wiss. Leipzig, Math-Phys. Kl.*, vol. 69, pp. 262–277, April 1917.

[6] R. O. Duda and P. E. Hart, "Use of the Hough Transformation to Detect Lines and Curves in Pictures," *Com. ACM*, vol. 15, no. 1, pp. 11–15, Jan. 1972.

[7] J. Illingworth and J. Kittler, "A Survey of the Hough Transform," *Computer Vision, Graphics, and Image Processing*, vol. 44, pp. 87–116, 1988.

[8] K. V. Hansen and J. Larsen, "An Algorithm for Successive Identification of Reflections," *IEEE Trans. IP*, vol. 3, no. 3, May 1994.

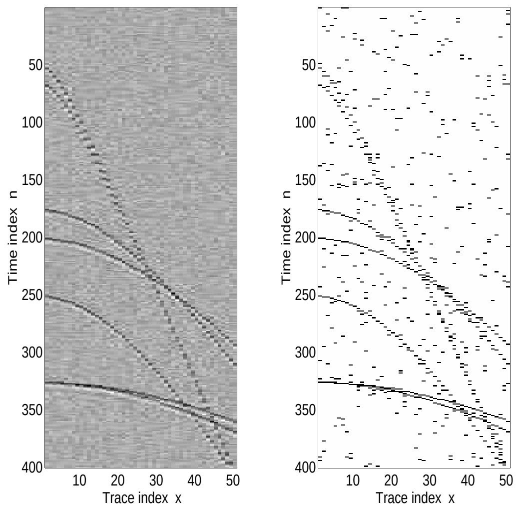

Figure 1: Left: CMP-gather. Right: Thresholded CMP-gather.

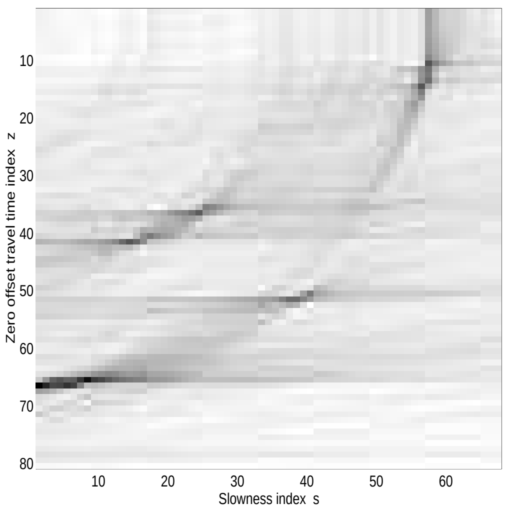

Figure 2: IPM-domain.

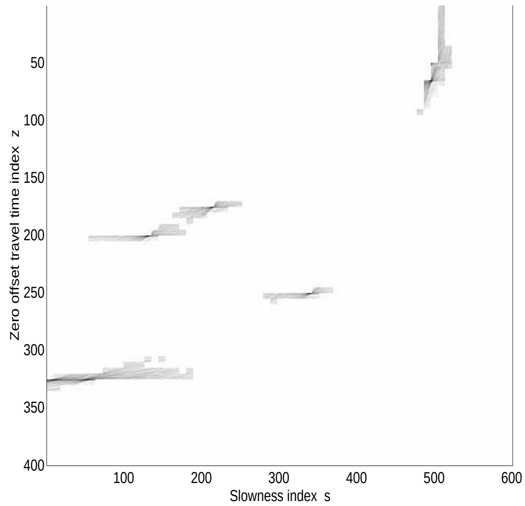

Figure 3: GRT-domain.

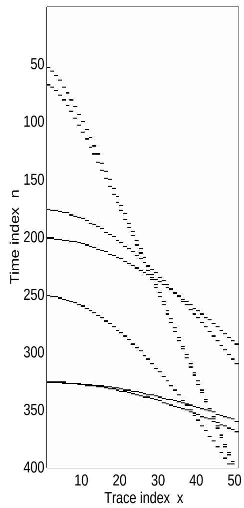

Figure 4: Identified reflection curves.